## Electronic Supplementary Information (ESI)

# Polymorphs, enantiomorphs, chirality and helicity in [Rh{*N,O*}($\eta^4$-cod)] complexes with {*N,O*} = salicylaldiminato Schiff base or aminocarboxylato ligands

**Christoph Janiak [a],*, Anne-Christine Chamayou [a], A. K. M. Royhan Uddin [b], Mohammed Uddin [c], Karl S. Hagen [c] and Mohammed Enamullah [b],***

[a] *Institut für Anorganische und Analytische Chemie, Universität Freiburg, Albertstr. 21, D-79104 Freiburg, Germany. E-mail: janiak@uni-freiburg.de; Fax: 49 761 2036147; Tel: 49 761 2036127*
[b] *Department of Chemistry, Jahangirnagar University, Dhaka-1342, Bangladesh. Email:enamullahju@yahoo.com; Fax: 8802-7791068; Tel: 8802-7791399*
[c] *Department of Chemistry, Emory University, Atlanta, GA 30322, USA.*

## Crystal pictures of 3R/3S and 3rac

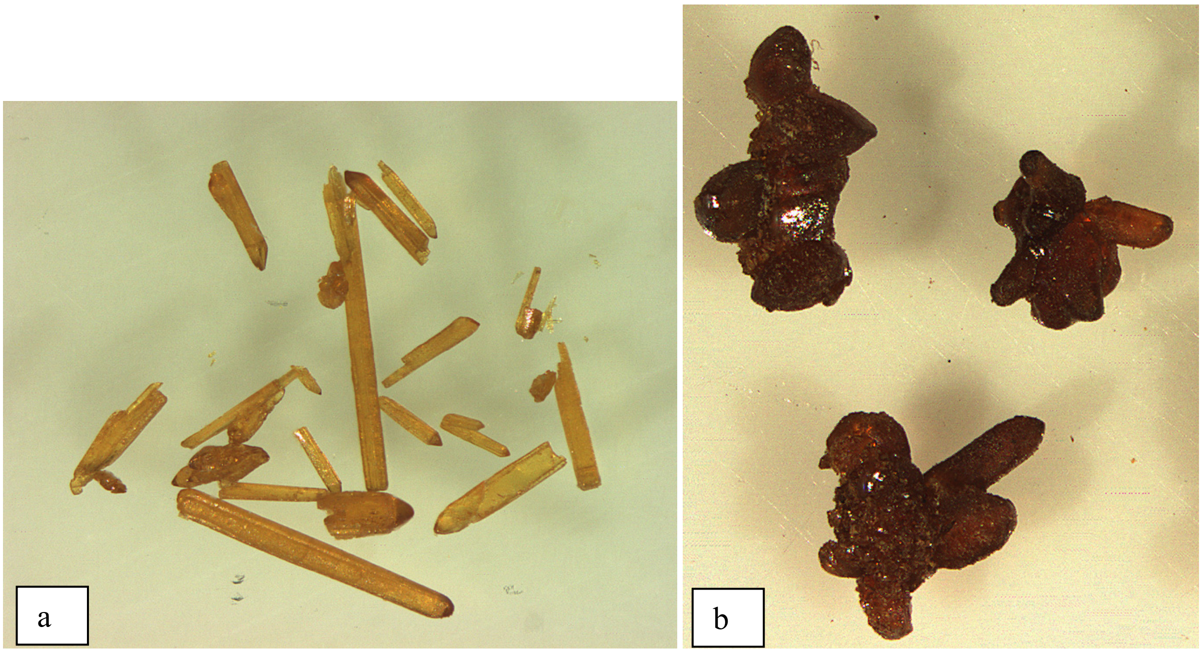

**Fig. S1** (a) Needle-shaped crystals of **3R** and **3S** (tetragonal $P4_3$ and $P4_1$, respectively); (b) block-shaped crystals of **3rac** (monoclinic $P2_1/c$).

## UV/VIS Absorption spectroscopy

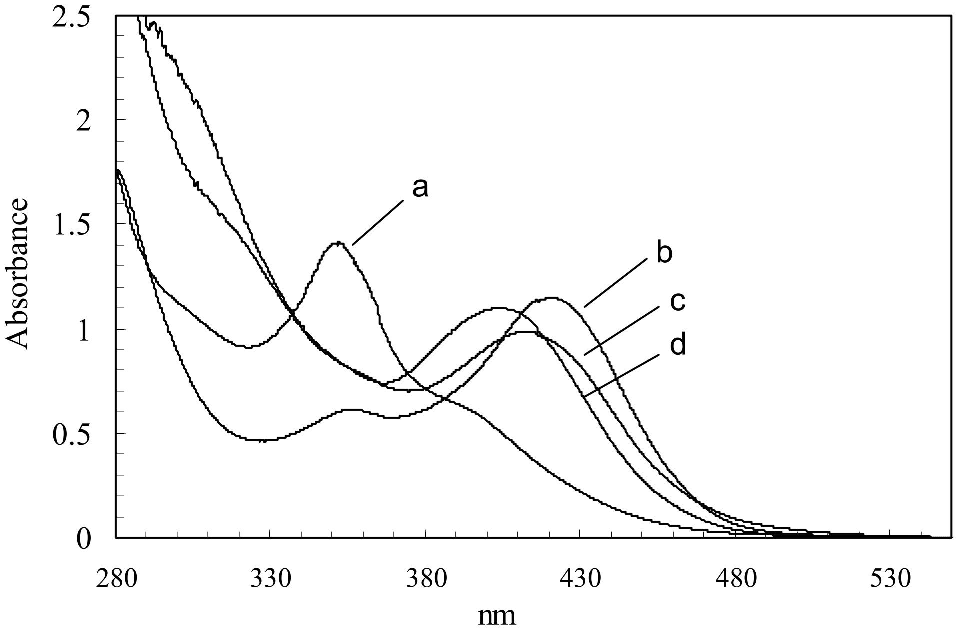

**Figure S2** UV-Vis. absorption spectra of (a) [RhCl(η$^4$-cod)]$_2$ (3.65·10$^{-4}$ mol·l$^{-1}$), (b) [Rh(O$_2$CMe)(η$^4$-cod)]$_2$ (2.98·10$^{-4}$ mol·l$^{-1}$), (c) [{Rh(η$^4$-cod)}$_2$(salen)] (**1**) (1.27·10$^{-4}$ mol·l$^{-1}$) and (d) [{Rh(η$^4$-cod)}$_2$(salophen)] (**2**) (1.22·10$^{-4}$ mol·l$^{-1}$) in $C_6H_6$ at 25 °C.

Figure S1 shows the absorption spectra of **1** and **2** together with those for [RhCl(η$^4$-cod)]$_2$ and [Rh(O$_2$CMe)(η$^4$-cod)]$_2$ for comparison studies. The spectral data are listed in Table S1 and their assignments are made based on the reported literature (see references in paper). The spectra of the Rh(η$^4$-cod)-Schiff base complexes are identical with each other and different from those of [RhCl(η$^4$-cod)]$_2$ and [Rh(O$_2$CMe)(η$^4$-cod)]$_2$ (Fig. S1).

The absorption spectrum of [RhCl(η$^4$-cod)]$_2$ shows three common characteristic bands: (i) a very strong band at higher energy (<320 nm), associated to the intra-ligand π→π* transition of (η$^4$-cod) moiety, (ii) a strong broad band at 330-380nm with absorption maximum at $\lambda_{max}$ = 352 nm ($\varepsilon_{max}$ = 3870 l·mol$^{-1}$·cm$^{-1}$), associated to the charge transfer (CT) transition based on the formation of the coordinative Rh-(η$^4$-cod)$^+$ bond and (iii) a broad shoulder at 380-500 nm ($\lambda_{max}$ ~396 nm), associated to the CT transition based on the formation of the more ionic [RhCl] bond. Similarly, spectrum of [Rh(O$_2$CMe)(η$^4$-cod)]$_2$ shows three separate bands, a very strong band at <320 nm for intra-ligand π→π* transition, a strong band at 330-380 nm with $\lambda_{max}$ = 356 nm ($\varepsilon_{max}$ = 2066 l·mol$^{-1}$·cm$^{-1}$), attributed to the CT due to [Rh(η$^4$-cod)]$^+$ and a relatively broad and stronger band at 380-500 nm ($\lambda_{max}$ = 421 nm, $\varepsilon_{max}$ = 3854 l·mol$^{-1}$·cm$^{-1}$) for CT transition between Rh(I) and acetate in the formation of [Rh(O$_2$CCH$_3$)].

A very strong band at higher energy (<360 nm), associated to the intra-ligand π→π* transitions of the imino group of the Schiff base in addition to the (η$^4$-cod) moiety, is observed in Rh(η$^4$-cod)-Schiff base complexes (see Table S1). Further, a strong broad band, observed at 400-500 nm ($\lambda_{max}/\varepsilon_{max}$ = 403 nm/8655 l·mol$^{-1}$·cm$^{-1}$ for **1**, 413 nm/8077 l·mol$^{-1}$·cm$^{-1}$ for **2**, 411 nm/13150 l·mol$^{-1}$·cm$^{-1}$ for **4** and 416 nm/3828 l·mol$^{-1}$·cm$^{-1}$ for **5**), is assigned to the ct transition between Rh(I) and diminato in the formation of [Rh(diminato)] (diminato = anion of Schiff base). However, the CT transition in the [Rh(η$^4$-cod)]$^+$ moiety likely shifts to higher energy and overlaps with the nearby very strong intra-ligand π→π* transitions, and are not detectable separately in Rh($\eta^4$-cod)-Schiff base complexes.

The absorption spectra demonstrate that the CT transition due to [Rh($\eta^4$-cod)]$^+$ moieties appears at almost the same positions in [RhCl($\eta^4$-cod)]$_2$ and [Rh($O_2$CMe)($\eta^4$-cod)]$_2$, while the transition due to [Rh(Cl/acetate)] moieties is found at different positions. These results are in good agreement with the idea of replacement of Cl$^-$ by acetate in [Rh($O_2$CMe)($\eta^4$-cod)]$_2$. However, the acetato ligand ($CH_3CO_2^-$) is further replaced by diminato in **1**, **2**, **4** and **5**, accompanied by a change in the corresponding CT bands of the absorption spectra (see Table S1 and Fig. S1).

**Table S1** UV/Vis spectral data of complexes **1**, **2**, **4**, **5** at 25 °C.[a]

| Complexes (concentrations) | π→π* transition | [Rh($\eta^4$-cod)] CT | [Rh(Cl/acetato/diminato)] CT |
|---|---|---|---|
| [($\eta^4$-cod)RhCl]$_2$<br>($3.65\cdot10^{-4}$ mol·l$^{-1}$)$^b$ | < 320 nm | 330-380 nm<br>$\lambda_{max}$ = 352 nm, $\varepsilon_{max}$ = 3870 | 380-500 nm<br>$\lambda_{max}$ ~396 nm (sh) |
| [Rh($\eta^4$-cod)($O_2CCH_3$)]$_2$<br>($2.98\cdot10^{-4}$ mol·l$^{-1}$)$^b$ | < 320 nm | 330-380 nm<br>$\lambda_{max}$ = 356 nm, $\varepsilon_{max}$ = 2066 | 380-500 nm<br>$\lambda_{max}$ = 421 nm, $\varepsilon_{max}$ = 3854 |
| [{Rh($\eta^4$-cod)}$_2$(salen)] (**1**)<br>($1.27\cdot10^{-4}$ mol·l$^{-1}$)$^b$ | < 360 nm | < 360 nm | 400-500 nm<br>$\lambda_{max}$ = 403 nm, $\varepsilon_{max}$ = 8655 |
| [{Rh($\eta^4$-cod)}$_2$(salophen)] (**2**)<br>($1.22\cdot10^{-4}$ mol·l$^{-1}$)$^b$ | < 360 nm | < 360 nm | 400-500 nm<br>$\lambda_{max}$ = 413 nm, $\varepsilon_{max}$ = 8077 |
| [Rh($\eta^4$-cod){(*R*)-*N*-(4-methoxphenyl)ethyl-2-oxo-1-naphthaldiminato-$\kappa^2$*N,O*}] (**4**)<br>($5.97\text{x}10^{-5}$ mol·l$^{-1}$)$^c$ | < 360 nm | < 360 nm | 400-500 nm<br>$\lambda_{max}$ = 411 nm, $\varepsilon_{max}$ = 13150 |
| [Rh($\eta^4$-cod){*N*-(*o*-toluene)-2-oxo-1-naphthaldiminato-$\kappa^2$*N,O*}] (**5**)<br>($2.12\cdot10^{-4}$ mol·l$^{-1}$)$^c$ | < 360 nm | < 360 nm | 400-500 nm<br>$\lambda_{max}$ = 416 nm, $\varepsilon_{max}$ = 3828 |

[a] Molar absorptivity ($\varepsilon_{max}$) values are in l·mol$^{-1}$·cm$^{-1}$; [b] in $C_6H_6$; [c] in $CH_2Cl_2$; sh = shoulder.

## Infrared spectroscopy

The most common characteristics IR-bands of the complexes are reported in the experimental section and their assignments are made based on the reported literature (see references in paper). The νC=N bands are observed at 1600-1620 cm$^{-1}$, while the νC=C occurs at 1578-1526 cm$^{-1}$ in Rh-Schiff base complexes. The aromatic νC–H bands are observed in the range of 3075-3000 cm$^{-1}$. Two new bands (which are absent in the free ligands) are observed around 675-680 cm$^{-1}$ and 459-465 cm$^{-1}$, which are assigned to the νRh-N and νRh-O, respectively.

Two very strong carbonyl bands are observed at 1561 cm$^{-1}$ (ν$CO_{2\ asy}$) and 1420 cm$^{-1}$ (ν$CO_{2\ sy}$) in the starting material [Rh(μ-$O_2$CMe)($\eta^4$-cod)]$_2$ and correspond to the bridging κ*O:O*'-coordination ($\eta^2$-coordination) of the carboxylate to the Rh(I) atom in the dimeric structure. These bands obviously disappeared in the prepared complexes. Further, the νO-H stretching band of the free Schiff bases (usually observed at 3250-3254 cm$^{-1}$) disappears in the Rh-Schiff base complexes, which indicates dissociation of the protic hydrogen and formation of a more ionic bond between Rh(I) and the hydroxyl oxygen atom.

The Rh-amino acid complex (**3**) shows two very strong carbonyl bands at 1625 cm$^{-1}$ (νCO$_{2\ \mathrm{asy}}$) and 1366 cm$^{-1}$ (νCO$_{2\ \mathrm{sy}}$), correspond to the κ*N,O*-coordination (η$^1$-CO$_2$ coordination) of the amino-carboxylate to the Rh(I) atom. This complex also exhibits the νN-H stretching bands at 3142 cm$^{-1}$ (νNH$_{\mathrm{asy}}$) and 3097 cm$^{-1}$ (νNH$_{\mathrm{sy}}$). Indeed, the absence of any νO-H stretching band (usually observed at 3450-3550 cm$^{-1}$ for hydrogen bonded O-H group of free amino acid) indicates the dissociation of the proton and formation of ionic bond between Rh(I) and the hydroxyl oxygen atom in **3**.

**Table S2** FT-IR spectral data of [Rh{*N,O*}(η$^4$-cod)] complexes (KBr, cm$^{-1}$).[a,b]

| Complexes | νO-H | νH-Ar | νC=N | νC=C | νC-O | νRh-N | νRh-O |
|---|---|---|---|---|---|---|---|
| [Rh(O$_2$CMe)(η$^4$-cod)]$_2$ | | - | - | | 1561vs,<br>1420vs | - | |
| H$_2$salen | 3254w | 3052w, 3010w, 2930w, 2901w, 2868w | 1636vs<br>1611vs | 1578vs, 1498s | - | - | - |
| [{Rh(η$^4$-cod)}$_2$(salen)] (**1**) | - | 3075w, 3049w, 3011m, 2930s, 2876m, 2829w | 1607vs | 1575sh 1530s | - | 677w | 462w |
| H$_2$salophen | 3250w | 3054s, 3010m, 2932s, 2880m, 2828w | 1613vs<br>1586s | 1561vs, 1482s | - | - | - |
| [{Rh(η$^4$-cod)}$_2$(salophen)] (**2**) | | 3075w, 3045w, 3019m, 2930s, 2874m, 2828w | 1609vs | 1578vs, 1526s | - | 675w | 460w |
| [Rh((*R*)-*N*-(4-methoxphenyl)ethyl-2-oxo-1-naphthaldimi-nato)(η$^4$-cod)] (**4**) | | 3066, 3042m | 1620vs | 1578vs | - | 675w | 465w |
| [Rh(*N*-(o-tolyl)-2-oxo-1-naphthaldimin-ato)(η$^4$-cod)] (**5**) | | 3047, 3010w | 1615,<br>1606vs | 1574, 1534vs | | 679w | 459w |

| Complexes | νN-H$_{\mathrm{asy}}$ | νN-H$_{\mathrm{sy}}$ | νH-Ar | νC-H | νCO$_2^-{}_{\mathrm{asy}}$ | δN–H | νCH$_2$ | νCO$_2^-{}_{\mathrm{sy}}$ |
|---|---|---|---|---|---|---|---|---|
| [Rh(*N*-phenylglyci-nato)(η$^4$-cod)] (**3rac**) | 3142m | 3097m | 3053s | 2943s | 1616vs | 1600s | 1491s | 1366s |

[a] KBr plates.

[b] vs: very strong, s: strong, m: medium, w: weak, sh shoulder.

## NMR spectroscopy

**Table S3** $^1$H NMR data (δ/ppm) for the olefinic protons in Rh{*N,O*}($\eta^4$-cod) complexes in CDCl$_3$.

| Complex | *trans* to N | | *trans* to O | | References |
|---|---|---|---|---|---|
| | 'left' | 'right' [a] | 'left' | 'right' [a] | |
| [{Rh($\eta^4$-cod)}$_2$(salen)] **1** | 4.40 (4.28 [d]) | | 3.58 (3.78 [d]) | | This work |
| [Rh(sal=N-*p*-tol)($\eta^4$-cod)] | 4.60 | | 3.20 | | 1 |
| [Rh(*o*-O$_2$NC$_6$H$_4$NH)($\eta^4$-cod)] | 4.46 | | 3.87 | | 2 |
| [(Rh($\eta^4$-cod))$_2$(dcbi)](NHEt$_3$) | 4.37 | | 4.05 | | |
| [Rh(*o*-aminophenolato)($\eta^4$-cod)] [d] | 4.16 | | 3.88 | | 4 |
| [Rh{(*R*)-*N*-(*p*-methoxphenyl)ethyl-2-oxo-1-naphthaldiminato}($\eta^4$-cod)] **4** | 4.61 | | 3.91 | | This work |
| [Rh(SB1)($\eta^4$-cod)] [e] | 4.54 | | 3.72 | | 5 |
| [Rh{*N,O*}($\eta^4$-cod)] [b] | 4.78 | | 3.33 | | 6 |
| [Rh(sal=N-*o*-tol)($\eta^4$-cod)] | 4.62 | | 3.34 | 2.66 | 1 |
| [(Rh($\eta^4$-cod))$_2$(salophen)] **2** | 4.54 | 4.37 | 3.53 | 2.45 | This work |
| [Rh{*N*-(*o*-tolyl)-2-oxo-1-naphthaldiminato}($\eta^4$-cod)] **5** | 4.59 | 4.53 | 3.32 | 2.62 | This work |
| [Rh($\mu$-hp/-mhp)($\eta^4$-cod)]$_2$ [c] | 5.38/5.33 | 5.11/5.04 | 4.12/4.28 | 3.29/2.91 | 7 |
| [(Rh($\eta^4$-cod))$_2$($\mu$-NH{*p*-tolyl})($\mu$-OMe)] [b] | 3.93 | 3.80 | 3.69 | 3.24 | 2 |
| [Rh(SB2)($\eta^4$-cod)] [f] | 4.50 | 4.42 | 4.29 | 3.73 | 5 |
| [Rh(*N*-phenylglycinato)($\eta^4$-cod)] **3** | | | 3.58 (3.60 [d]) | | This work, 8 |
| [Rh(*L*-methylglycinato)($\eta^4$-cod)] [d] | | | 3.92 | | 8 |
| [Rh(*o*-aminobenzoato)($\eta^4$-cod)] [d] | | | 3.93 | | 4 |

[a] 'left' and 'right' is an arbitrary assignment for olefin protons to either side of a plane bisecting the C=C bond. [b] in benzene-d$_6$; [c] in toluene-d$_8$; [d] in dmso-d$_6$. [e] SB1 = (*R*)-*N*-1-(phenyl)ethylsalicylaldiminato. [f] SB2 = (*R*)-*N*-1-(2-methoxphenyl)ethylsalicylaldiminato.

---

[1] N. Platzer, N. Goasdoue and R. Bonnaire, *J. Organomet. Chem.*, 1978, **160**, 455.

[2] C. Tejel, M. A. Ciriano, M. Bordonaba, J. A. Lopez, F. J. Lahoz and L. A. Oro, *Inorg. Chem.*, 2002, **41**, 2348.

[3] J. C. Bayon, G. Net, P. G. Rasmussen and J. B. Kolowich, *J. Chem. Soc., Dalton Trans.*, 1987, 3003-3007.

[4] M. Enamullah, A.K.M. Royhan Uddin and M. Uddin, *J. Bangladesh Chem. Soc.*, 2008, in press.

[5] M. Enamullah, A. K. M. Royhan Uddin, A. C. Chamayou and C. Janiak, *Z. Naturforsch.*, 2007, **62b**, 807-817.

[6] R. Aumann, I. Goettker-Schnetmann, R. Froehlich and P. Saarenketo, C. Holst, *Chem. Eur. J.*, 2001, **7**, 711..

[7] G. S. Rodman and K. R. Mann, *Inorg. Chem.*, 1988, **27**, 3338.

[8] M. Enamullah, A. Sharmin, M. Hasegawa, T. Hoshi, A.-C. Chamayou and C. Janiak, *Eur. J. Inorg. Chem.*, 2006, 2146.

**Table S4** $^{13}$C NMR spectral data (δ/ppm) and $J(^{103}\mathrm{Rh}\text{-}^{13}\mathrm{C})$/Hz in the cod region in Rh{*N,O*}(η$^4$-cod) complexes in $CDCl_3$.

| Complex | Methylene carbons (singlets) | Olefin carbons (doublets) ($J(^{103}\mathrm{Rh}\text{-}^{13}\mathrm{C})$ in parentheses) | | | | Ref. |
|---|---|---|---|---|---|---|
| | | *trans* to N | | *trans* to O | | |
| | | 'left' | 'right' [a] | 'left' | 'right' [a] | |
| [(Rh(η$^4$-cod))$_2$(salen)] **1** | 31.7, 28.8 | 85.5 (11.9) | | 71.2 (14.2) | | Tw |
| [(Rh(η$^4$-cod))$_2$(salen)] | 31.8, 28.8 | 85.5 (12.5) | | 71.2 (15.0) | | 1 |
| [Rh(*o*-$O_2NC_6H_4NH$)(η$^4$-cod)] | 31.1, 29.4 | 84.4 (11.0) | | 71.8 (11.0) | | 2 |
| [(Rh(η$^4$-cod))$_2$(dcbi)](NHEt$_3$) | 31.2, 30.0 | 82.7 (13.0) | | 71.7 (14.0) | | 3 |
| [Rh(*o*-aminophenolato)(η$^4$-cod)] [d] | 30.4br, 29.5br | 79.6br | | 68.9br | | 4 |
| [(Rh(η$^4$-cod))$_2$(salophen)] **2** | 32.6, 30.3, 29.5, 27.9 | 85.8 (11.7) | 84.3 (11.8) | 74.3 (14.6) | 69.7 (14.4) | Tw |
| [(Rh(η$^4$-cod))$_2$(salophen)] | 32.5, 30.3, 29.5, 27.9 | 85.8 (12.5) | 84.3 (12.5) | 74.3 (12.5) | 69.7 (15.0) | 1 |
| [Rh{(*R*)-*N*-(4-methoxphenyl)ethyl-2-oxo-1-naphthaldiminato}(η$^4$-cod)] **4** | 31.8, 31.1, 28.9, 28.3 | 84.7 (11.8) | 84.1 (11.7) | 73.3 (14.2) | 71.1 (14.3) | Tw |
| [Rh{*N*-(*o*-tolyl)-2-oxo-1-naphthaldiminato}(η$^4$-cod)] **5** | 30.7, 30.3, 28.2, 27.9 | 83.7 (12.2) | 83.2 (11.8) | 73.4 (14.1) | 72.3 (14.1) | Tw |
| [Rh(SB1)(η$^4$-cod)] [e] | 32.5, 32.0,29.6, 29.2 | 85.7 (12.1) | 85.3 (12.3) | 73.5 (14.2) | 71.4 (14.6) | 5 |
| [Rh{*N,O*}(η$^4$-cod)] [b] | 32.1, 31.9, 29.6, 29.5 | 81.6 | 81.3 | 75.4 | 75.1 | 6 |
| [Rh(μ-hp/-mhp)(η$^4$-cod)]$_2$ [c] | 35.0, 33.0, 30.1, 29.0<br>/33.4, 32.1, 30.5, 29.2 | 89.1<br>/87.7 | 77.2<br>/76.6 | 74.4<br>/72.8 | 70.9<br>/72.2 | 7 |
| [(Rh(η$^4$-cod))$_2$(μ-NH{*p*-tolyl})(μ-OMe)] [b] | 32.7, 32.2, 29.4, 29.0 | 80.1 (12.0) | 78.6 (13.0) | 73.9 (14.0) | 70.2 (15.0) | 2 |
| [Rh(*N*-phenylglycinato)(η$^4$-cod)] **3** | 30.1<br>29.7 [d] | 78.2br<br>77.9br [d] | | | | Tw<br>8 |
| [Rh(*L*-methylglycinato)(η$^4$-cod)] [d] | 30.1 | 79.6br | | 72.1br | | 8 |
| [Rh(*o*-aminobenzoato)(η$^4$-cod)] [d] | 29.6 | 77.1br | | | | 4 |

[a] 'left' and 'right' is an arbitrary assignment for the olefin carbons to either side of a plane bisecting the C=C bond. [b] in benzene-$d_6$. [c] in toluene-$d_8$. [d] in dmso-$d_6$. [e] SB1 = (*R*)-*N*-1-(phenyl)ethylsalicylaldiminato. [f] SB2 = (*R*)-*N*-1-(2-methoxphenyl)ethylsalicylaldiminato. br = broad signal. Tw = This work.

## Rh-cod bond distances

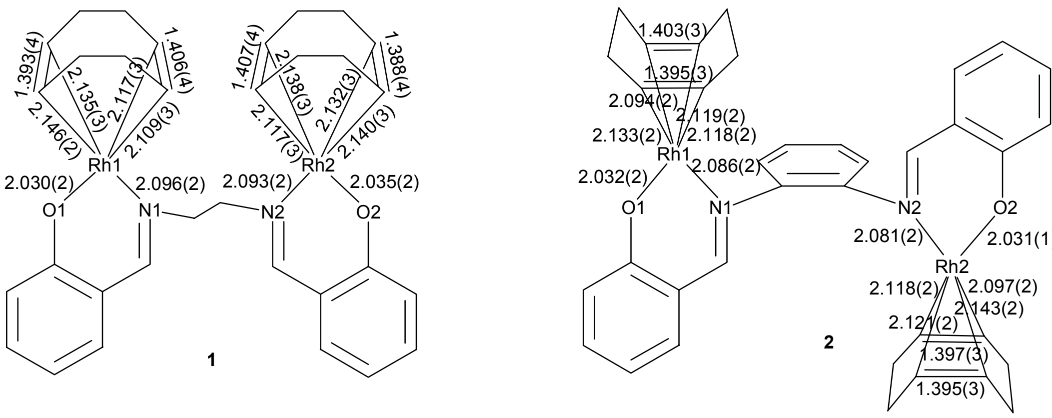

**Scheme S1** Bond distances (Å) for Rh–$C_{cod}$, C=$C_{cod}$, Rh–N and Rh–O in **1** and **2** to document the slightly asymmetrical binding of the cyclooctadiene (cod) ligands due to the different *trans* nitrogen or oxygen donor atoms.

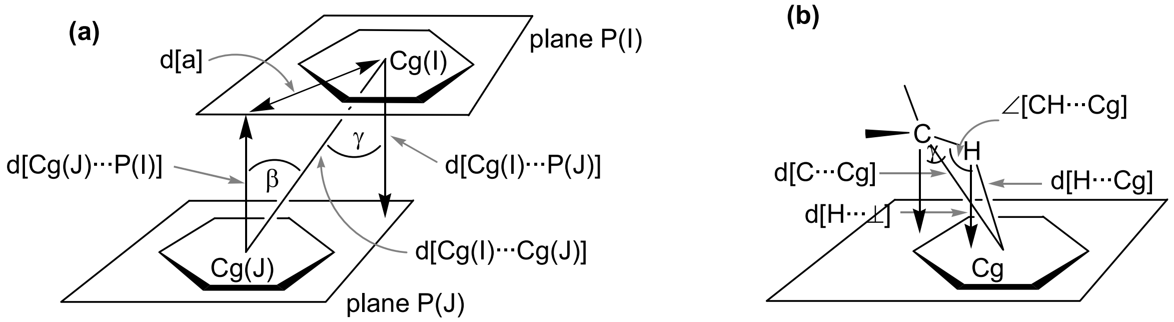

**Scheme S2** Graphical presentation of the parameters used in Table S5 for the description of (a) π-π stacking and (b) CH-π interactions.

## Supramolecular π-π and CH-π interactions

**Table S5** Distances (d/Å) and angles (°) for the π-contacts in the crystal structures of **1**, **2**, **4** and **5**. [a]

| **π-π interactions**<br>compound,<br>ring(I)···ring(J) | d[Cg(I)···Cg(J)] [b] | α [c] | β [d] | γ [e] | d[Cg(I)···P(J)] [f] | d[Cg(J)···P(I)] [g] | d[a] [h] |
|---|---|---|---|---|---|---|---|
| **1**, | | | | | | | |
| Rh1-metallacycle···Rh1-metallacycle$^{2}$<br>Rh1-O1C4C3C2N1·· Rh1-O1C4C3C2N1$^{2}$ | 3.99 | 0 | 32.5 | 32.5 | 3.37 | 3.37 | 2.15 |
| Rh2-metallacycle···Rh2-metallacycle$^{2'''}$<br>Rh2-O2C20C19C18·· Rh2O2C20C19C18$^{2'''}$ | 3.85 | 0 | 24.8 | 24.8 | 3.50 | 3.50 | 1.62 |
| Symmetry transformations: 2 = 1–x, –y, –z; 2’’’ = 2–x, 1–y, 1–z. | | | | | | | |

| **CH-π interactions**<br>compound,<br>ligand-C-H···ring | d[H···Cg] [i] | d[H···⊥] [j] | γ [k] | ∠[CH···Cg] [l] | d[C···Cg] [m] |
|---|---|---|---|---|---|
| **1**, | | | | | |
| C1–H1A···ringC3$^{2}$–C8$^{2}$ | 2.62 | 2.60 | 6.8 | 159 | 3.56 (see Fig. S2) |
| C15–H15B···(Rh2O2C20C19C18)$^{2'}$ | 2.79 | 2.62 | 19.7 | 131 | 3.51 (see Fig. S3) |
| C27–H27A···ringC3$^{2''}$–C8$^{2''}$ | 2.94 | 2.88 | 12.4 | 141 | 3.76 (see Fig. S4) |
| Symmetry transformations: 2 = 1–x, –y, 2’ = 2–x, –y, –z; 2’’ = 2–x, –y, 1–z. | | | | | |
| **2a**, | | | | | |
| C32–H32B···(Rh1O1C13C8C7N1)$^{1}$ | 2.86 | 2.61 | 24.3 | 167 | 3.83 (see Fig. S5) |
| Symmetry transformations: 1 = 1+x, y, z. | | | | | |
| **2b** (Refcode SCLIRB10), | | | | | |
| C3–H3A···(Rh1O1C9C14C15N1)$^{3}$ | 2.74 | 2.70 | 9.4 | 151 | 3.62 (see Fig. S6) |
| C8–H8B···ringC9$^{3}$–C14$^{3}$ | 2.73 | 2.73 | 0.6 | 165 | 3.67 (see Fig. S6) |
| Symmetry transformations: 3 = –0.5+x, 1–y, 0.5–z. | | | | | |
| **4**, | | | | | |
| C9–H9C···(RhO1C1C6C7N)$^{4}$ | 2.70 | 2.57 | 17.7 | 146 | 3.54 (see Fig. S7) |
| C17–H17A···(RhO1C1C6C7N)$^{4'}$ | 2.64 | 2.62 | 6.9 | 175 | 3.58 (see Fig. S7) |
| Symmetry transformations: 4 = 1–x, –0.5+y, 0.5–z; 4’ = 2–x, 0.5+y, 0.5–z. | | | | | |
| **5**, | | | | | |
| C22–H22···(RhOC1C6C7N)$^{2}$ | 2.84 | 2.80 | 9.22 | 132 | 3.53 |
| Symmetry transformations: 2 = x, 1–y, –0.5+z. | | | | | |

[a] For a graphical depiction of distances and angles in the assessment of the π-contacts, see Scheme S2. Pyridyl rings of the terpy or bipy ligands are named by their nitrogen atoms. – [b] Centroid-centroid distance. – [c] Dihedral angle between the ring planes. – [d] Angle between the centroid vector Cg(I)···Cg(J) and the normal to the plane I ("slip angle"). – [e] Angle between the centroid vector Cg(I)···Cg(J) and the normal to the plane J. – [f] Perpendicular distance of Cg(I) on ring plane J. – [g] Perpendicular distance of Cg(J) on ring plane I. – [h] Slippage; distance between Cg(I) and perpendicular projection of Cg(J) on Ring I; parallel displacement between ring centroids from a perfect face-to-face alignment. –
[i] H–centroid distance. – [j] Perpendicular distance of H on ring plane. – [k] Angle between the C-H vector and the normal to the π-plane. – [l] C-H···centroid angle. – [m] C···centroid distance.

Compounds not listed in Table S5 contain no or only π-stacking interactions which can be viewed as medium to weak in that they exhibit rather long centroid-centroid distances (Cg···Cg> 4.0 Å) together with large slip angles (*β*, *γ* > 30°) and vertical displacements (*d* > 2.0 Å). In comparison, strong π-stackings show rather short centroid-centroid contacts (< 3.8 Å), small slip angles (*β*, *γ* < 25°) and vertical displacements (*d* < 1.5 Å) which translate into a sizable overlap of the aromatic planes.

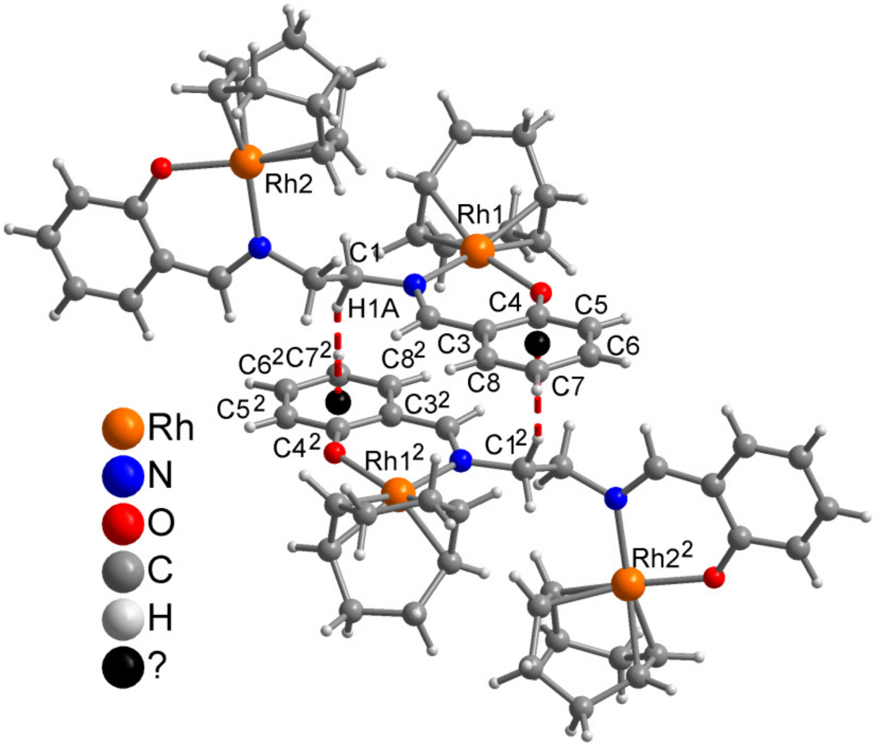

**Fig. S3** Complementary contacts C1–H1A···ringC3$^2$–C8$^2$ (red dashed lines) in compound **1**.

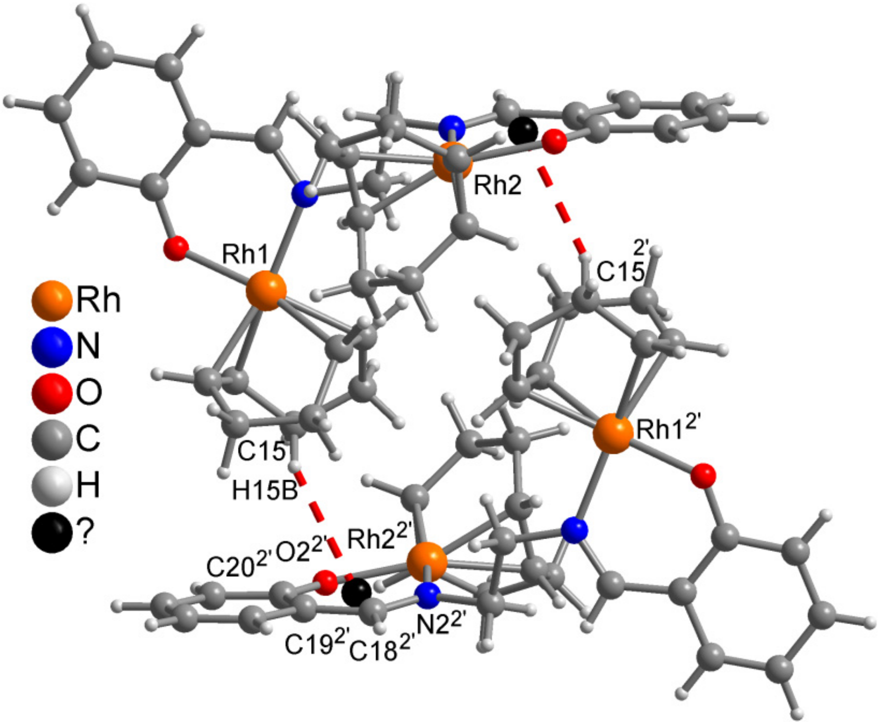

**Fig. S4** Complementary contacts C15–H15B···(Rh2O2C20C19C18)$^{2’}$ (red dashed lines) in compound **1**.

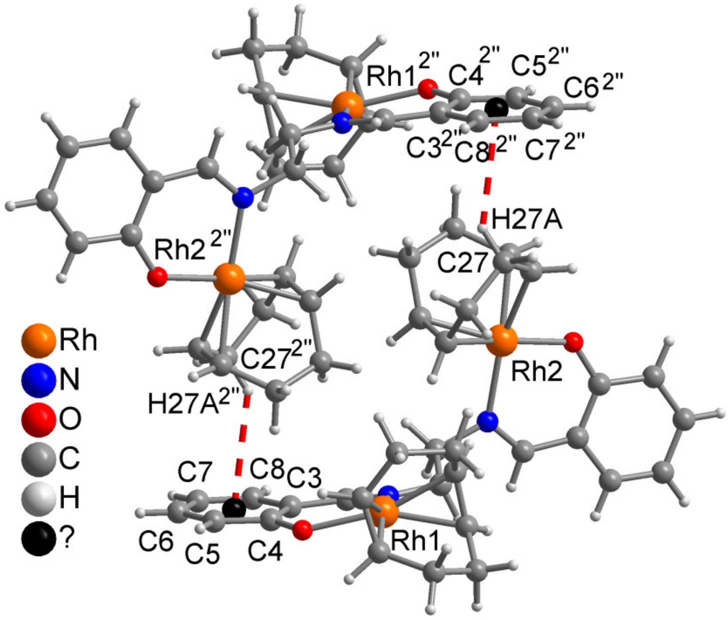

**Fig. S5** Complementary contacts C27–H27A···ringC3$^{2''}$–C8$^{2''}$ (red dashed lines) in compound **1**.

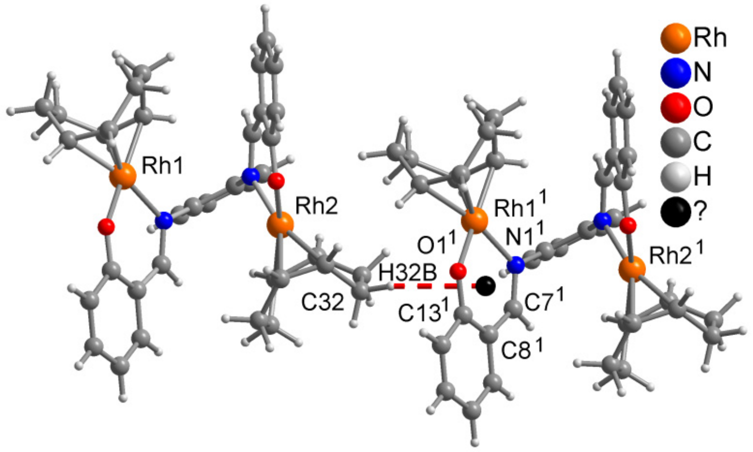

**Fig. S6** Contact C32–H32B···(Rh1O1C13C8C7N1)$^1$ (red dashed line) in compound **2a**.

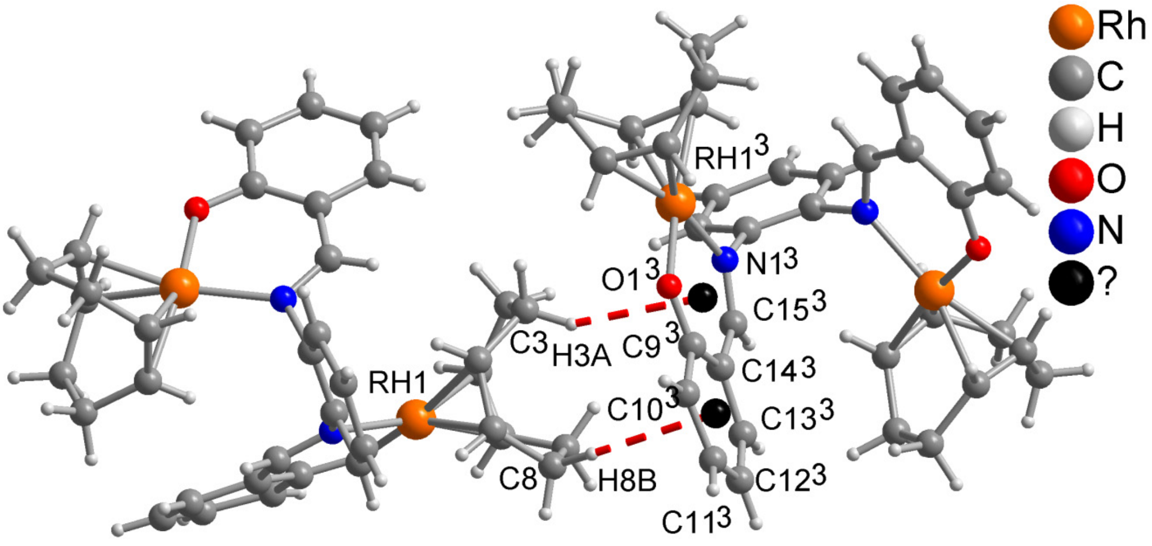

**Fig. S7** Contacts C3–H3A···(Rh1O1C9C14C15N1)$^1$ and C8–H8B···ringC9$^3$–C14$^3$ (red dashed lines) in compound **2b**.

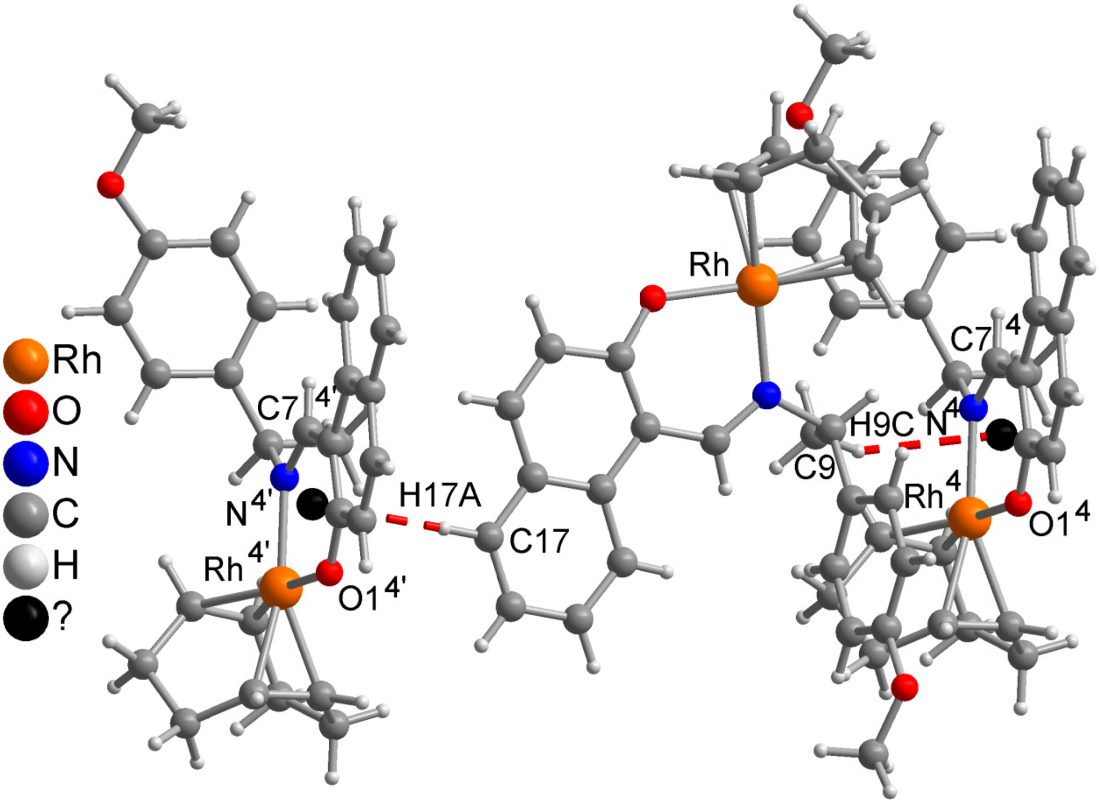

**Fig. S8** Contacts C9–H9C···(RhO1C1C6C7N)$^{4}$ and C17–H17A···(RhO1C1C6C7N)$^{4'}$ (red dashed lines) in compound **4**.

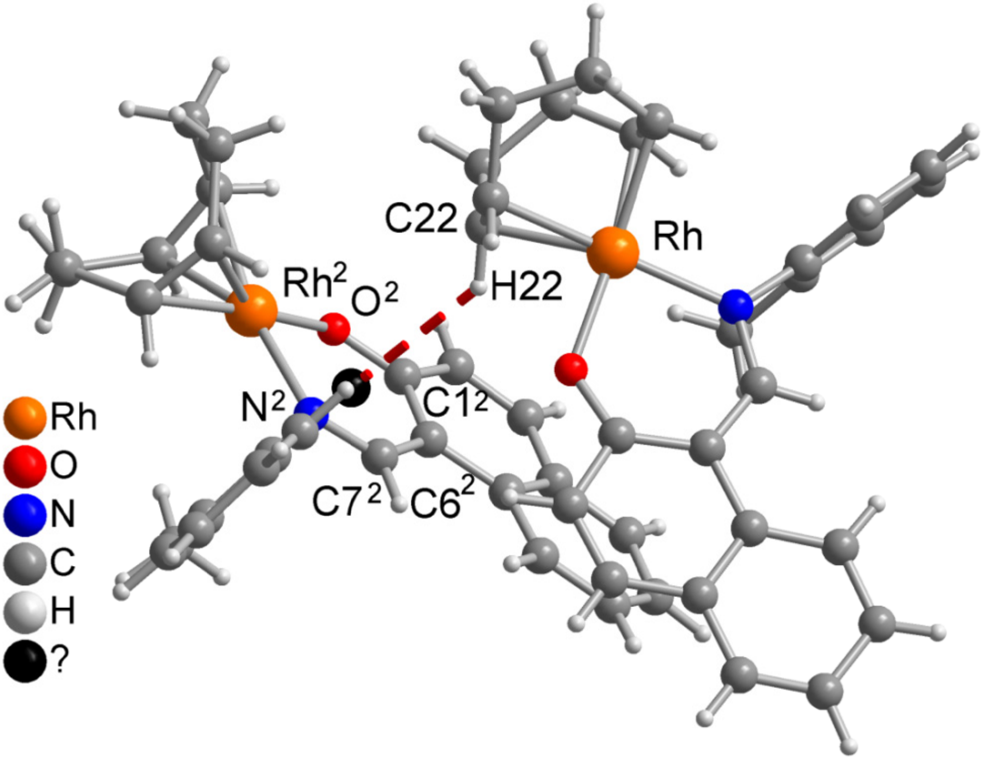

**Fig. S9** Contact C22–H22···(RhOC1C6C7N)$^{2}$ (red dashed line) in compound **5**.